# Mathematical Description of the Shape of Conical Hydrometeors

PAO-KUAN WANG

*Department of Meteorology, University of Wisconsin, Madison 53706*

(Manuscript received 20 May 1982, in final form 19 July 1982)

ABSTRACT

A mathematical function is presented to approximate the shape of conical hydrometeors such as conical graupel and hailstones and large falling raindrops. The function provides a method of parametric classification of conical hydrometeors. Steps and examples of fitting to real conical hydrometeors are given. The examples demonstrate that this function closely approximates the shape of these particles. Formulas for calculating the axial cross-sectional area, volume and area of the surface of revolution are given. The function will be useful in the future study of the physical properties of conical hydrometeors.

## 1. Introduction

The shape of cloud and precipitation particles is one of the most important microphysical properties in cloud physics. Particles of different shapes falling in air may have different flow fields around them and, therefore, may be subject to different hydrodynamic drags. These drag forces have significant influences on the microphysical behavior of these particles, such as their fall velocities, surface heat dissipation rates and collision efficiencies with other particles (Pruppacher and Klett, 1978). The shape is also one of the most important factors affecting the backscattering of radar waves by particles (Atlas *et al.*, 1953; Battan, 1973).

Many hydrometeors have complicated shapes, such as hexagonal columns, plates, and dendrites for ice crystals, cones and spheroids for graupel and hailstones, and near-oblate-spheroids for large raindrops. These shapes often make the analysis of physical properties difficult. One often has to approximate these shapes by other simpler shapes, for example, large raindrops by oblate spheroids, ice columns by circular cylinders and ice plates by thin oblate spheroids. The approximations are made so that simple mathematical formulas can be used to describe the shapes of these particles. In this paper we want to investigate the conical-shaped hydrometeors.

There are two main kinds of conical hydrometeors: conical graupel and hailstones; and large raindrops. Barge (1972; quoted by Battan, 1973) investigated a total of 1920 hailstones and reported that 21% of them were of conical shape while 41, 10, and 8% were oblate, spherical and prolate, respectively. Although the fraction of conical hailstones was not the largest, it is large enough to deserve some special attention. Many graupel are also conical, as reported by Knight and Knight (1970), Locatelli and Hobbs (1974) and Hobbs (1974), among others. Falling raindrops of millimeter size usually have near-oblate-spheroid shapes with a more-or-less round top and flattened bottom (Pruppacher and Klett, 1978). Under certain conditions, such as in a strong vertical electric field, drops can be elongated to become pear-shaped (Pruppacher *et al.*, 1982; Richards and Dawson, 1971). They can also be thought of as conical particles.

Conical graupel and hailstones can be approximated by spherical sectors, or the combination of a flat-based cone and a spherical cap, as has been done by Jayaweera and Mason (1965) and List and Schemenauer (1971). While these approximations are certainly workable, and indeed much has been learned by making such assumptions, they also have some shortcomings. For example, these approximations all consist of two surfaces, conical and spherical. This may cause some difficulties for theoretical study of these particles because the two surfaces constitute a mixed boundary problem, which is usually more difficult to solve. The shapes of falling raindrops have been investigated theoretically by Pruppacher and Pitter (1971). They used a cosine series to represent the shape of a deformed drop. Their method is necessary for the determination of drop shape under the influence of certain forces. On the other hand, for some studies of physical properties, such as the heat diffusion rates from such drops and the flow fields around them, it may be desirable to have a simpler mathematical function instead of a series to describe their shape.

This paper presents a single mathematical function which can describe the shapes of conical graupel and hailstones and some deformed raindrops. It will be shown in later sections that this function does approximate many conical hydrometeors. This function

0022-4928/82/112615-08$06.00

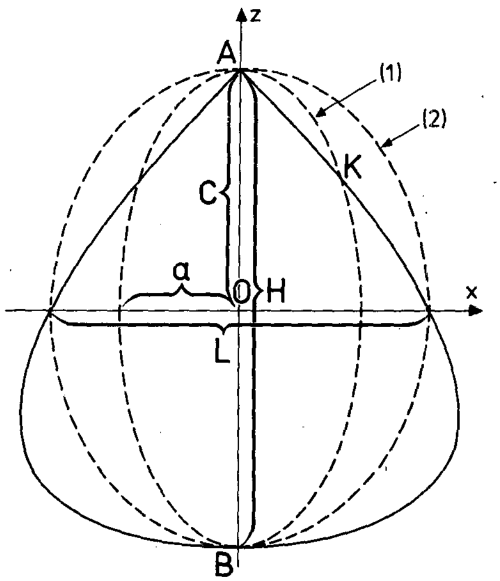


FIG. 1. Definition of the coordinate system and various quantities. Solid curve is an axial cross-section of a conical body. Dashed curves (1) and (2) are the generating ellipse and limiting ellipse, respectively.

allows us to calculate the volume, cross-sectional area and the area of surface of revolution of these hydrometeors. The parameters involved in this function may also serve as a method of classifying the dimensions of these hydrometeors.

## 2. Mathematical formulation

The mathematical function in consideration is

$$x = \pm a[1 - (z^2/C^2)]^{1/2} \cos^{-1}(z/\lambda C), \tag{1}$$

where $x$ and $z$ are values of horizontal and vertical coordinates of the surface, respectively (see Fig. 1); $a$, $C$ and $\lambda$ are parameters to be determined. $a$ and $C$ have dimensions of length, whereas $\lambda$ is a dimensionless number. $C$ is one-half the length from the apex to the bottom, along the $z$-axis; the center point is defined as the origin $O$. $a$ is defined in the following. We first note that

$$x = \pm a[1 - (z^2/C^2)]^{1/2} \tag{2}$$

is the equation of an ellipse whose semi-axes in the $x$- and $z$-directions are $a$ and $C$, respectively. Therefore, Eq. (1) can be thought of as an ellipse modified by an arccosine function. We may conveniently call the ellipse of Eq. (2) the *generating ellipse*. Therefore, $a$ is the horizontal semi-axis of the generating ellipse.

The principal value of the arccosine function lies between 0 and $\pi$, i.e.,

$$0 \leqslant \cos^{-1}(z/\lambda C) \leqslant \pi. \tag{3}$$

Also, since the absolute value of a cosine function cannot be larger than one, and since $-C \leqslant z \leqslant C$, it is necessary that

$$\lambda \geqslant 1. \tag{4}$$

We need not consider the negative values of $\lambda$, since $z$ can be either positive or negative. When $\lambda \rightarrow \infty$, $(z/\lambda C) = 0$ and

$$\cos^{-1}(z/\lambda C) \cos^{-1}(0) = \frac{\pi}{2}, \tag{5}$$

Eq. (1) becomes

$$x = \pm \frac{\pi}{2} a[1 - (z^2/C^2)]^{1/2}, \tag{6}$$

which is the equation of an ellipse with horizontal and vertical semi-axes $\pi a/2$ and $C$, respectively. Since it represents the case when $\lambda$ becomes very large, it may be conveniently called the *limiting ellipse*. Curves representing Eqs. (1), (2) and (6) are shown in Fig. 1. We see that Eq. (1) is a pear-shaped curve. It will be shown later that Eq. (1) can approximate the shape of conical hydrometeors. The curve in Fig. 1 represents an axial cross-section only. To obtain a three dimensional body, it is only necessary to rotate the curve about the $z$-axis.

## 3. Fitting steps and examples

Various conical shapes can be obtained by changing parameters $a$, $C$ and $\lambda$ in Eq. (1). In the following, we outline the steps which determine $a$, $C$ and $\lambda$ for a real conical hydrometeor. We use a conical graupel as an example here.

### a. *Step 1*

First we should determine $C$. This is obtained by measuring the length $H$ from the apex $A$ to the bottom point $B$ (refer to Fig. 1). $C$ is one half of this length. The center point $O$ is defined as the origin. Line $H$ is also the $z$-axis.

### b. *Step 2*

Next we determine $a$. First draw the $x$-axis and measure the length $L$, as shown in Fig. 1. Of course, $z = 0$ along the $x$-axis. Therefore, from Eq. (1), we have

$$L = 2x = 2a[1 - (z^2/C^2)]^{1/2} \cos^{-1}(z/\lambda C),$$

when $z = 0$ and $L = a\pi$, so that

$$a = L/\pi. \tag{7}$$

### c. *Step 3*

Finally we have to determine $\lambda$. This can be divided into two cases:

### 1) The conical curve intersects with the generating ellipse

This is probably the most common case for conical graupel and hailstones. In this case, the function

$$\cos^{-1}(z/\lambda C),$$

is smaller than 1 for some values (usually positive) of $y$. At the point of intersection ($K$ in Fig. 1), the value of the arccosine function

$$\cos^{-1}(z_K/\lambda C) = 1,$$

where $z_K$ is the $z$-coordinate of point $K$. Thus,

$$z_K/\lambda C = \cos(1) = 0.5403.$$

Therefore,

$$\lambda = z_K/0.5403C. \tag{8}$$

Hence, putting in the values of $z_K$ and $C$, the value of $\lambda$ is determined.

Note that the value of $\lambda$ determined from Eq. (8) may be slightly less than 1 due to measuring errors or deviation from standard shape. In this case, we have to set $\lambda = 1$ since, by definition, the argument of the arccosine function

$$z_K/\lambda C \leqslant 1.$$

However, this small correction does not produce a large deviation from the actual shape.

### 2) The conical curve does not intersect with the generating ellipse

In this case, $\cos^{-1}(z/\lambda C) \geqslant 1$ along the conical curve. We can determine the value of $\lambda$ from its relation with the maximum value of $x$-coordinate, $x_m$. In the following, we only have to consider the half curve

$$x = a[1 - (z^2/C^2)]^{1/2} \cos^{-1}(z/\lambda C),$$

since the curve is symmetrical with respect to the $z$-axis. The maximum $x$ value, $x_m$, will occur at the point where

$$\left.\frac{dx}{dz}\right|_{\substack{x=x_m\\ z=z_m}} = 0$$

$$= \left\{-\frac{az}{C^2}\frac{\cos^{-1}(z/\lambda C)}{[1-(z^2/C^2)]^{1/2}} - \frac{a[1-(z^2/C^2)]^{1/2}}{(\lambda^2C^2 - z^2)^{1/2}}\right\}_{\substack{x=x_m\\ z=z_m}}, \tag{9}$$

where $z_m$ is the $z$-coordinate of the maximum point. Eq. (9) can be written as

$$\left.\begin{aligned} &\left\{\frac{z}{C^2}\frac{a[1-(z^2/C^2)]^{1/2}\cos^{-1}(z/\lambda C)}{[1-(z^2/C^2)]} + \frac{a}{C}\frac{[1-(z^2/C^2)]^{1/2}}{[\lambda^2-(z^2/C^2)]^{1/2}}\right\}_{x_m,z_m} = 0 \\ &\left\{\frac{z_m}{C^2}\frac{a[1-(z_m^2/C^2)]^{1/2}\cos^{-1}(z_m/\lambda C)}{[1-(z_m^2/C^2)]} + \frac{a}{C}\frac{[1-(z_m^2/C^2)]^{1/2}}{[\lambda^2-(z_m^2/C^2)]^{1/2}}\right\}_{x_m} = 0 \end{aligned}\right\}. \tag{10}$$

But

$$a[1-(z_m^2/C^2)]^{1/2}\cos^{-1}(z_m/\lambda C) = x_m, \tag{11}$$

$$1 - (z_m^2/C^2) = x_g^2/a^2, \tag{12}$$

where $x_g$ is the $x$-coordinate of the generating ellipse when $z = z_m$. Putting (11) and (12) into (10), we have

$$x_m z_m a^2/C^2 x_g^2 = -\frac{1}{C}\frac{x_g}{[\lambda^2 - (z_m^2/C^2)]^{1/2}},$$

$$\lambda^2 - (z_m^2/C^2) = (Cx_g^3/x_m z_m a^2)^2.$$

Thus

$$\lambda = [(Cx_g^3/x_m z_m a^2)^2 + (z_m/C)^2]^{1/2}. \tag{13}$$

As in case 1), the value of $\lambda$ determined from (13) may be subject to errors and deviations and may occasionally be smaller than one. In this case, we have to set $\lambda = 1$. It is also possible to construct a numerical routine to determine $a$, $C$ and $\lambda$ by digital computer, but we won't consider this method here.

Sometimes it is desirable to calculate $x_m$ and $z_m$ from a given set of parameters $a$, $c$ and $\lambda$. This is given in Section 5d.

## 4. Examples and discussions

Using the above steps, I have tried to fit many conical graupel and hailstones which appeared in the literature. Fig. 2 shows two examples taken from Mason (1971) and Iribarne and Cho (1979). It appears that the fittings by Eq. (1) are reasonably close to the actual shapes. It also appears that the most common values of $\lambda$ lie between 1 and 2. Fig. 3 shows an example of fitting for a falling large raindrop, in an environment with and without a vertical electric field. The photographs are taken from Pruppacher *et al.* (1982).

Note that Eq. (1) can also be used to describe spheres and spheroids. In these cases, we artificially set $\cos^{-1}(z/\lambda C) = 1$. The remaining equation then describes an ellipse. By rotating the ellipse about the $z$-axis we obtain spheroids. If $a < C$, prolate spheroids result. If $a > C$, oblate spheroids result. In the special case where $a = C$, spheres result.

While Eq. (1) appears to be a reasonably good approximation to many conical hydrometeors, one also

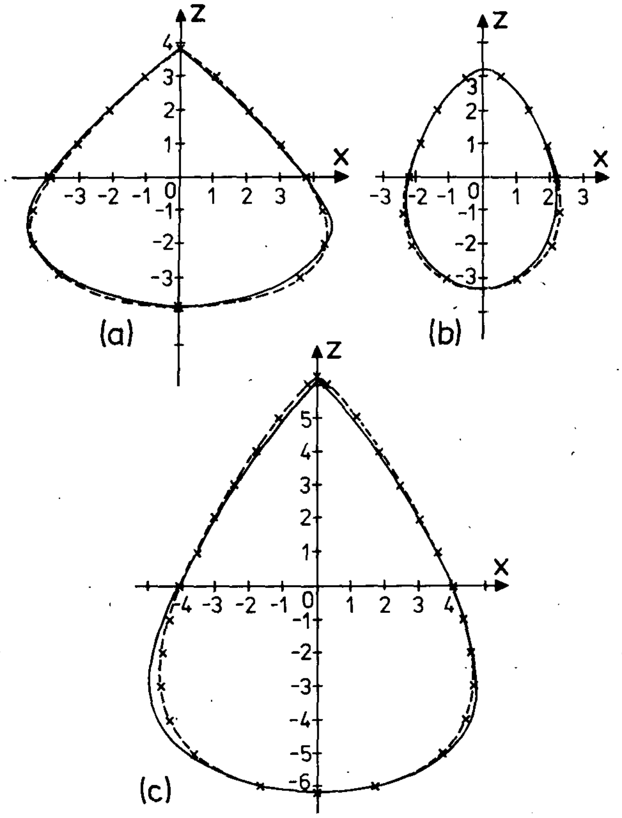


FIG. 2. Examples of fitting conical graupels and hailstones by Eq. (1). (a) $a = 2.42$, $C = 3.80$, $\lambda = 1.0$; (b) $a = 1.40$, $C = 3.20$, $\lambda = 1.72$; (c) $a = 2.55$, $C = 6.20$, $\lambda = 1.045$. (a) and (b) are from Mason (1971, Figs. 6.20 and 6.21), (c) is from Iribarne and Cho (1980, Fig. V-21). The actual dimension (mm) of $a$ and $C$ can be obtained by dividing the numbers by scale factors. The scale factor is 1.639 for (a) and (b), and 1.575 for (c).

may note that it represents an idealized approximation. Natural conical hydrometeors, especially conical graupel and hailstones, may differ considerably from the idealized conical shape. They may not possess rotational symmetry and may have a rough surface. However, in many simple theoretical studies, such complications can be disregarded, at least to a first order of approximation. Eq. (1) also provides a convenient way to categorize the dimensions of observed conical hydrometeors.

As mentioned before, some conical hydrometeors may have shapes that deviate considerably from Eq. (1). However, some of them can be described in a similar manner to Eq. (1), i.e., an ellipse modified by some functions. Figs. 4 and 5 are two examples. Fig. 4 represents a teardrop whose generating equation is

$$x = \pm a[1 - (z^2/C^2)]^{1/2}[1 - (z/C)], \quad (14)$$

and Fig. 5 represents another teardrop whose generating equation is

$$x = \pm a[1 - (z^2/C^2)]^{1/2}[1 - (\tan^{-1} z/\tan^{-1} C)]. \quad (15)$$

## 5. Cross-sectional area, volume and area of the surface of revolution

The cross-sectional area, volume and area of the surface of revolution are among the most important quantities which determine the physical properties of hydrometeors such as liquid/solid water contents, heat and vapor diffusion rates, etc. We can use Eq. (1) to estimate the above geometrical quantities for conical hydrometeors. One may refer to Courant and John (1965) for the formula used below.

### *a. Cross-sectional area*

We restrict ourselves here to the calculation of axial cross-sectional area of a conical hydrometeor. This area is

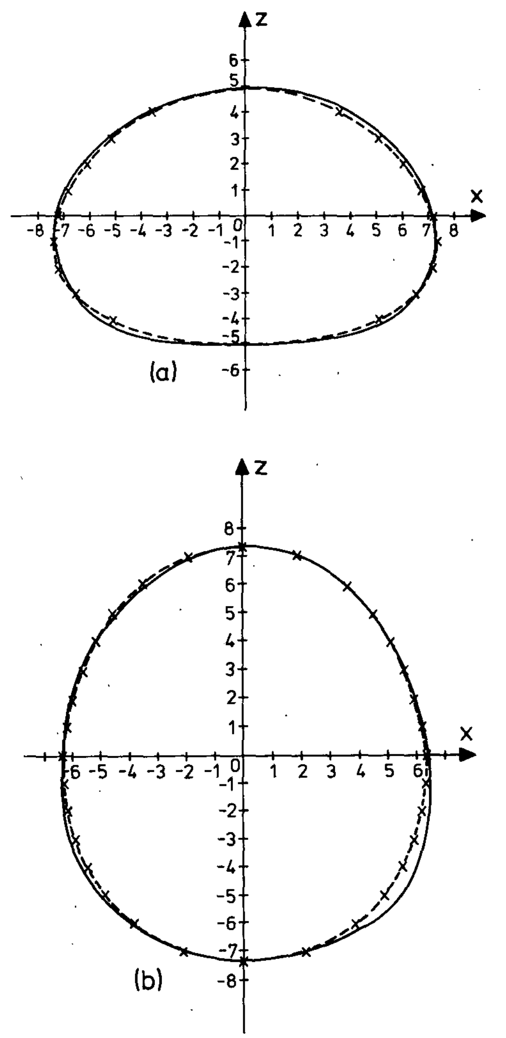


FIG. 3. Examples of fitting large freely-falling water drops by Eq. (1). (a) A freely-falling drop of radius 2.3 mm, $a = 4.58$, $C = 5.0$, $\lambda = 14.79$. (b) The same drop as in (a) but falling in a vertical electric field of $E_0 = 7.75$ kV cm$^{-1}$, $a = 4.01$, $C = 7.50$, $\lambda = 75.11$. Both from Pruppacher *et al.* (1982). The scale factor is 2.

$$A = 2\int_{-c}^{c} x dz$$

$$= 2a\int_{-c}^{c}\left(1-\frac{z^2}{C^2}\right)^{1/2}\cos^{-1}(z/\lambda C)dz. \quad (16)$$

It turns out that this area is independent of $\lambda$ and the result is

$$A = \pi^2 aC/2. \quad (17)$$

The calculation is given in Appendix A.

*b. Volume*

While the axial cross-sectional area is independent of $\lambda$, the volume does depend on $\lambda$. The volume is given by

$$V = \int_{-c}^{c} \pi x^2 dz$$

$$= \pi a^2 \int_{-c}^{c}\left(1-\frac{z^2}{C^2}\right)\left[\cos^{-1}\left(\frac{z}{\lambda C}\right)\right]^2 dz. \quad (18)$$

The detail of the calculation is given in Appendix B. The results are

$$V = 3.6167\pi a^2 C, \quad \lambda = 1, \quad (19)$$

$$V = 3.2889\pi a^2 C, \quad \lambda = \infty, \quad (20)$$

$$V \approx \pi^2 aC\left(\beta_0 + \frac{\beta_2}{\lambda^2} + \frac{\beta_4}{\lambda^4} + \frac{\beta_6}{\lambda^6} + \frac{\beta_8}{\lambda^8} + \frac{\beta_{10}}{\lambda^{10}}\right),$$

$$1 < \lambda < \infty, \quad (21)$$

where

$$\left.\begin{matrix} \beta_0 = 3.2889, & \beta_2 = 0.2667, & \beta_4 = 0.0382 \\ \beta_6 = 0.0113, & \beta_8 = 0.0046, & \beta_{10} = 0.0024 \end{matrix}\right\}. \quad (22)$$

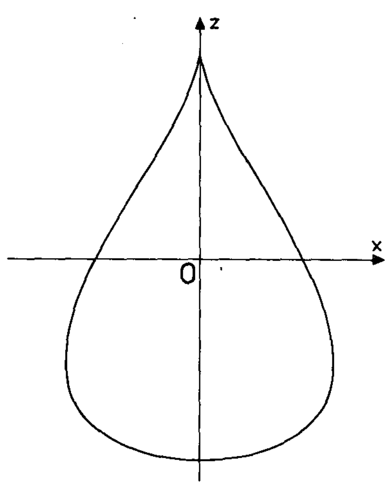


FIG. 4. A "teardrop" generated by Eq. (14). $a = 5$, $C = 10$. Arbitrary units.

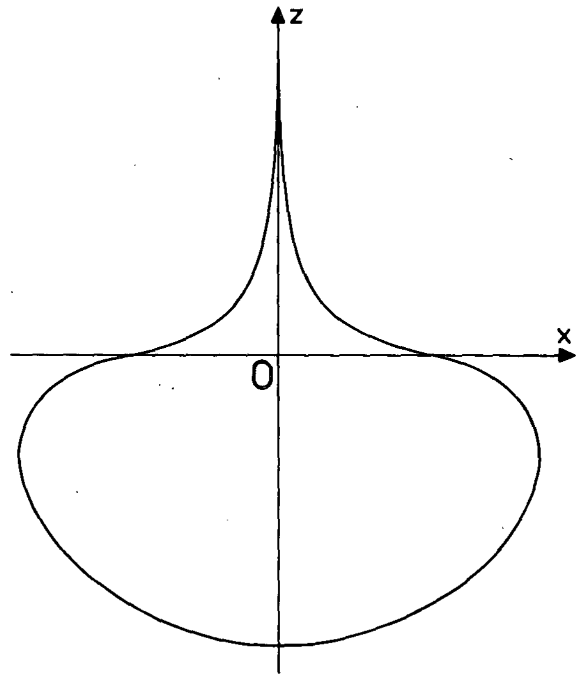


FIG. 5. A distorted "teardrop" generated by Eq. (15). $a = 5$, $C = 10$. Arbitrary units.

Since $\lambda \geqslant 1$, the largest error that can occur in using Eq. (21) is when $\lambda = 1$. But even in this case, the volume calculated from Eq. (21) is

$$V_{\lambda=1} = 3.6121\pi a^2 C,$$

which deviates from Eq. (19) by only 0.13%. In view of the approximate nature of using Eq. (1) as the shape of the conical hydrometeor, this error is completely negligible.

*c. Area of the surface of revolution*

The area of the surface of revolution can be calculated from Guldins' rule:

$$A_r = 2\pi\int_{-c}^{c} x\left[1+\left(\frac{dx}{dz}\right)^2\right]^{1/2} dz. \quad (23)$$

This equation can be transformed into

$$A_r = -2\pi aC\lambda\int_{\cos^{-1}(-1/\lambda)}^{\cos^{-1}(1/\lambda)}$$

$$\times\, v\left\{f(v)\sin^2 v + \frac{a^2}{\lambda^2 C^2}\left[\frac{\lambda^2}{2} v \sin 2v + f(v)\right]^2\right\}^{1/2} dv$$

$$= -2\pi aC\lambda I_r, \quad (24)$$

where

$$v = \cos^{-1}(z/\lambda C), \quad (25)$$

$$f(v) = 1 - \lambda^2\cos^2 v. \quad (26)$$

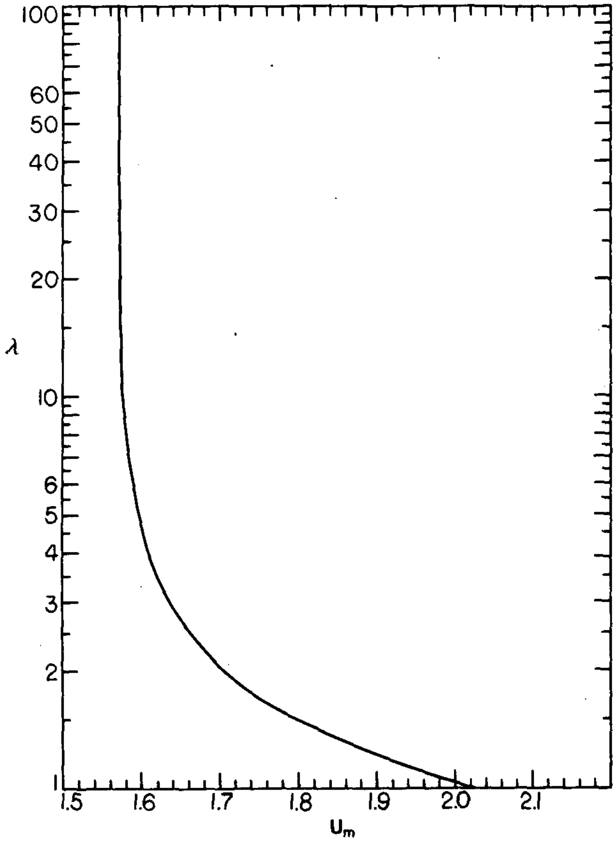


FIG. 6. Values of λ and the corresponding $u_m$ from Eq. (30).

The integral $I_r$ in Eq. (24) was carried out by numerical method and the result is surprisingly simple. For λ up to as large as $10^5$, $I_r$ is almost exactly equal to $(-\pi/\lambda)$. Therefore, for the normal range of λ (usually close to 1), the area of the surface of revolution is almost exactly

$$A_r = -2\pi aC\lambda\left(-\frac{\pi}{\lambda}\right) = 2\pi^2 aC, \qquad (27)$$

to a very high degree of accuracy. However, numerical calculation does show that $I_r$ decreases slowly with increasing λ. As λ becomes infinity, the area $A_r$ becomes

$$A_{r,\infty} = \pi^2 a\left(\frac{\pi a}{2} + \frac{\sin^{-1}KC}{K}\right), \qquad (28)$$

where

$$K^2 = \left(\frac{1}{C^2} - \frac{\pi^2 a^2}{4C^4}\right). \qquad (29)$$

Eq. (28) can be easily checked by setting $\lambda \to \infty$ and $C = \pi a/2$. Then, the second term in the braces vanishes and we have a sphere with surface area $4\pi C^2 = \pi^3 a^2 = 2\pi^2 aC$. $A_{r,\infty}$ is smaller than $2\pi^2 aC$. For example, if we let $a = 5$ mm, $C = 10$ mm, then $A_{r,\infty} = 919.7$ mm$^2$, whereas $2\pi^2 aC = 986.96$ mm$^2$, a difference of 6.8%. Again, in view of the fact that these are all approximations, we can probably live with this error.

*d. Cross-sectional area normal to the direction of fall*

The cross-sectional area normal to the direction of fall is one of the important dynamical quantities of conical particles. If the conical particle falls in the direction of its axis of symmetry, this area is simply $\pi x_m^2$, where $x_m$ was defined in Section 3. The formulation in Section 3 is for determining $a$, $C$ and λ, from a photo of a particle. Here we shall investigate a converse problem, namely, determining $x_m$ and $z_m$ for a given set of $a$, $C$ and λ. The most straightforward method will be by putting Eqs. (9) and (1) directly into the computer and solving for $z_m$ and $x_m$ by an iterative method. In the following, we provide an alternative method.

We first note that the value of $z_m$ (and thus the corresponding $x_m$) must be such that Eq. (9) holds. By letting $\cos u_m = (z_m/\lambda C)$, we can transform Eq. (9) into:

$$u_m \cos u_m \sin u_m - \cos^2 u_m = \frac{1}{\lambda^2}, \quad 0 \leq u_m \leq \pi, \qquad (30)$$

while at the same time one must remember that $\lambda^2 \cos^2 u_m \leq 1$.

The possible solutions of $u_m$ are in the range between $\pi/2$ (when $\lambda \to \infty$) and 2.028758 (when $\lambda = 1$). Fig. 6 gives a curve of λ versus $u_m$. Thus, for a given λ, we can find a corresponding value of $u_m$. The value of $z_m$ is then given by

$$z_m = \lambda C \cos u_m . \qquad (31)$$

Putting this $z_m$, along with $a$, $C$ and λ, into Eq. (1), we obtain $x_m$. As an example, the conical graupel in Fig. 2b has $a = 1.40$, $C = 3.20$ and $\lambda = 1.72$. From Fig. 6, the value of $u_m$ corresponding to $\lambda = 1.72$ is 1.75. Thus

$$z_m = (1.72)(3.20)\cos(1.75) = -0.9811,$$

and from Eq. (1) the corresponding $x_m$ is

$$x_m = (1.40)\left[1 - \left(\frac{-0.9811}{3.20}\right)^2\right]^{1/2}(1.75) = 2.3320.$$

$x_m$ is related to the characteristic lengths used by several previous investigators in describing conical particles. For example, Jayaweera (1971) used a characteristic length $L^*$, defined by Pasternak and Gauvin (1960), which is the ratio of the total surface area divided by its perimeter $P$ normal to the flow. In terms of $a$, $C$ and λ, this would be equivalent to

$$L^* = \frac{A_r}{2\pi x_m} = \frac{2\pi^2 aC}{2\pi x_m} = \frac{\pi aC}{x_m}. \qquad (32)$$

Other investigators, such as List and Schemenauer (1971) and Heymsfield (1978) used a characteristic length which is essentially $2x_m$.

## 6. Conclusions

In the above we have used Eq. (1) to approximate the shapes of conical hydrometeors. By specifying various values of the parameters $a$, $C$ and $\lambda$, we can generate different kinds of conical shapes. If a conical hydrometeor can be approximated by Eq. (1) with rotation about the $z$-axis, then its axial cross-sectional area, volume and area of the surface of revolution are given by formulas in Section 5. This will allow a more systematic classification of conical hydrometeors and a convenient way of estimating the water content and other physical quantities of the hydrometeor.

Needless to say, the actual conical hydrometeors are much more complicated. Various features such as surface roughness and highly asymmetric shape always make perfect approximation impossible. But as the above examples have shown, the approximation by Eq. (1) is very close in many cases.

Perhaps the most desirable property of Eq. (1) is that it is a single function, not a combination of two functions such as a line and a circle. This allows us to treat the surface of revolution of Eq. (1) as a coordinate. If we can establish an orthogonal coordinate system, by finding two other orthogonal surfaces, this coordinate system will be very useful for studying the dynamics of conical bodies. This research is currently underway.

*Acknowledgments.* The author would like to thank the anonymous reviewers for very useful suggestions and Ms. Eva Singer and Ms. Debbie Schiess for typing the manuscript. This research is partially supported by University of Wisconsin Graduate Research Fund 120223 and by the United States Environmental Protection Agency, under assistance agreement number R809371-01-0. Although the research described in this article has been funded in part by EPA, it has not been subject to the Agency's required peer and administrative review and, therefore, does not reflect the view of the Agency and no official endorsement should be inferred.

### APPENDIX A

### Area of an Axial Cross-section

Eq. (16) gives

$$A = 2\int_{-c}^{c} xdz = 2a\int_{-c}^{c}\left(1-\frac{z^2}{C^2}\right)^{1/2}\cos^{-1}\left(\frac{z}{\lambda C}\right)dz.$$

If we let $u = z/C$, then

$$A = 2aC\int_{-1}^{1}(1-u^2)^{1/2}\cos^{-1}\left(\frac{u}{\lambda}\right)du. \quad (33)$$

Let

$$I = \int_{-1}^{1}(1-u^2)^{1/2}\cos^{-1}\left(\frac{u}{\lambda}\right)du. \quad (34)$$

Since $|u| \leqslant 1$, $|u|/\lambda \leqslant 1$, we can expand the arccosine function into an infinite series of $(u/\lambda)$:

$$\begin{aligned}\cos^{-1}\left(\frac{u}{\lambda}\right) &= \frac{\pi}{2} - \left[\sum_{n=0}^{\infty}\frac{(2n-1)!!}{(2n)!(2n+1)}\left(\frac{u}{\lambda}\right)^{2n+1}\right] \\ &= \frac{\pi}{2} - \left[\left(\frac{u}{\lambda}\right) + \frac{1}{2\cdot 3}\left(\frac{u}{\lambda}\right)^3 + \frac{1\cdot 3}{2\cdot 4\cdot 5}\left(\frac{u}{\lambda}\right)^5 + \frac{1\cdot 3\cdot 5}{2\cdot 4\cdot 6\cdot 7}\left(\frac{u}{\lambda}\right)^7 + \cdots\right] \\ &= \frac{\pi}{2} - \left[\left(\frac{1}{\lambda}\right)u + \left(\frac{0.167}{\lambda^3}\right)u^3 + \left(\frac{0.0752}{\lambda^5}\right)u^5 + \left(\frac{0.0446}{\lambda^7}\right)u^7 + \cdots\right]. \quad (35)\end{aligned}$$

Putting (32) into (31), we obtain

$$I = \frac{\pi}{2}\int_{-1}^{1}(1-u^2)^{1/2}du - \left(\frac{1}{\lambda}\right)\int_{-1}^{1}u(1-u^2)^{1/2}du - \left(\frac{0.167}{\lambda^3}\right)\int_{-1}^{1}u^3(1-u^2)^{1/2}du + \cdots. \quad (36)$$

But for $m = 2n + 1 (n = 0, 1, 2, \cdots)$,

$$\int_{-1}^{1}u^m(1-u^2)^{1/2}du = -\frac{1}{(m+2)} \times \{u^{m-1}[(1-u^2)^{1/2}]^3\}_{-1}^{1} - (m-1)\int_{-1}^{1} \times u^{m-2}(1-u^2)^{1/2}du = 0 \quad (37)$$

(see, for example, Dwight, 1961). Therefore,

$$I = \frac{\pi}{2}\int_{-1}^{1}(1-u^2)^{1/2}du = \frac{\pi}{2}\left[\frac{u(1-u^2)^{1/2}}{2} + ½\sin^{-1}u\right]_{-1}^{1} = \frac{\pi^2}{4}$$

and

$$A = 2aCI = (\pi^2/2)aC. \quad (38)$$

Eq. (38) can be easily checked for two special cases, namely, $\lambda = 1$ and $\lambda = \infty$.

*a.* $\lambda = 1$

In this case we let $v = \cos^{-1}u$. Then

$$I = \int_{-1}^{1}(1-u^2)^{1/2}\cos^{-1}udu = -\int_{\pi}^{0}v\sin^2 vdv = -\left(\frac{v^2}{4} - \frac{v\sin 2v}{4} - \frac{\cos 2v}{8}\right)_{\pi}^{0} = \frac{\pi^2}{4}.$$

Thus

$$A_{\lambda=1} = \frac{\pi^2}{2}aC. \quad (39)$$

*b.* $\lambda = \infty$

In this case,

$$\cos^{-1}(u/\lambda) = \cos^{-1}(0) = \pi/2$$

and

$$I = \frac{\pi}{2}\int_{-1}^{1}(1-u^2)^{1/2}du = -\frac{\pi}{2}\int_{\pi}^{0}\sin^2 v$$

$$= -\frac{\pi}{2}\left(\frac{v}{2}-\frac{\sin^2 v}{4}\right)_{\pi}^{0} = \frac{\pi}{4}.$$

Thus

$$A_{\lambda=\infty} = \frac{\pi^2}{2}aC. \quad (40)$$

## APPENDIX B

## Calculation of Volume

Eq. (18) gives

$$V = \pi a^2\int_{-C}^{C}\left(1-\frac{z^2}{C^2}\right)\left[\cos^{-1}\left(\frac{z}{\lambda C}\right)\right]^2 dz$$

$$= \pi a^2 C\int_{-1}^{1}(1-u^2)\left[\cos^{-1}\left(\frac{u}{\lambda}\right)\right]^2 du, \quad (41)$$

where $u = z/C$. We investigate three cases of $\lambda$:

*a.* $\lambda = 1$

Eq. (38) becomes (letting $v = \cos^{-1}u$)

$$V = \pi a^2 C\int_{-1}^{1}(1-u^2)(\cos^{-1}u)^2 du$$

$$= -\pi a^2 C\int_{\pi}^{0} v^2\sin^3 v dv$$

$$= \pi a^2 C\left(\frac{1}{27}-\frac{\pi^2}{12}-3+\frac{3}{4}\pi^2\right) = 3.6167\pi a^2 C.$$

*b.* $\lambda = \infty$

Eq. (38) becomes

$$V = \pi a^2 C\left(\frac{\pi}{2}\right)^2\int_{-1}^{1}(1-u^2)du = \frac{\pi^3}{4}a^2 C(2-2/3)$$

$$= \frac{\pi^2}{3}\pi a^2 C = 3.2889\pi a^2 C.$$

*c.* $1 < \lambda < \infty$

In this case we expand $\cos^{-1}(u/\lambda)$ as in Eq. (32). The square of it gives

$$\left[\cos^{-1}\left(\frac{u}{\lambda}\right)\right]^2 = \frac{\pi^2}{4}-\left(\frac{\pi}{\lambda}\right)u + \left(\frac{1}{\lambda^2}\right)u^2 - \left(\frac{0.167\pi}{\lambda^3}\right)u^3 + \left(\frac{0.334}{\lambda^4}\right)u^4 - \left(\frac{0.0752\pi}{\lambda^5}\right)u^5 + \left(\frac{0.1783}{\lambda^6}\right)u^6 - \cdots. \quad (42)$$

Eq. (38) then becomes

$$V = \pi a^2 C\int_{-1}^{1}(1-u^2)\left[\frac{\pi^2}{4}-\left(\frac{\pi}{\lambda}\right)u+\left(\frac{1}{\lambda^2}\right)u^2 - \left(\frac{0.167\pi}{\lambda^3}\right)u^3 + \left(\frac{0.334}{\lambda^4}\right)u^4 - \cdots\right]du.$$

Integration of terms with odd powers of $u$ in the square bracket yields even functions of $u$ which therefore vanish. Only terms with even powers of $u$ survive. The result is

$$V = \pi a^2 C\left[3.2889 + \frac{0.2667}{\lambda^2} + \frac{0.0382}{\lambda^4} + \frac{0.0113}{\lambda^6} + \frac{0.0046}{\lambda^8} + \frac{0.0024}{\lambda^{10}} + \cdots\right]. \quad (43)$$

If we neglect higher-order terms, we see that Eq. (43) is identical with Eq. (21).

## REFERENCES


Atlas, D., M. Kerker and W. Hitchfeld, 1953: Scattering and attenuation by non-spherical atmospheric particles. *J. Atmos. Terr. Phys.*, **3,** 108–119.

Battan, L. J., 1973: *Radar Observation of the Atmosphere.* University of Chicago Press, 324 pp.

Courant, R., and F. John, 1965: *Introduction to Calculus and Analysis*, Vol. I. Wiley-Interscience, 661 pp.

Dwight, H. B., 1961: *Tables of Integrals and Other Mathematical Data.* Macmillan, 336 pp.

Heymsfield, A. J., 1978: The characteristics of graupel particles in northeastern Colorado cumulus congestus clouds. *J. Atmos. Sci.*, **35,** 284–295.

Hobbs, P. V., 1974: *Ice Physics.* Oxford University Press, 837 pp.

Iribarne, J. V., and H. R. Cho, 1980: *Atmospheric Physics.* D. Reidel, 212 pp.

Jayaweera, K. O. L. F., and B. J. Mason, 1965: The behavior of freely falling cylinders and cones in a viscous fluid. *J. Fluid Mech.*, **22,** 709–720.

——, 1971: Calculations of ice crystal growth. *J. Atmos. Sci.*, **28,** 728–736.

Knight, C. A., and N. C. Knight, 1970: The falling behavior of hailstones. *J. Atmos. Sci.*, **27,** 672–681.

List, R., and R. S. Schemenauer, 1971: Free-fall behavior of planar snow crystals, conical graupel, and small hail. *J. Atmos. Sci.*, **28,** 110–115.

Locatelli, J. D., and P. V. Hobbs, 1974: Fall speeds and masses of solid precipitation particles. *J. Geophys. Res.*, **79,** 2185–2197.

Mason, B. J., 1971: *The Physics of Clouds*, 2nd ed. Oxford University Press, 671 pp.

Pasternak, I. S., and W. H. Gauvin, 1960: Turbulent heat and mass transfer from stationary particles. *Can. J. Chem. Eng.*, **38,** 35–42.

Pruppacher, H. R., and J. D. Klett, 1978: *Microphysics of Clouds and Precipitation.* D. Reidel, 714 pp.

——, and R. L. Pitter, 1971: A semi-empirical determination of the shape of cloud and raindrops. *J. Atmos. Sci.*, **28,** 86–94.

——, R. Rasmussen, C. Walcek and P. K. Wang, 1982: A wind tunnel investigation of the shape of uncharged raindrops in the presence of an external, vertical electric field. *Proc. Second Int. Colloq. on Drops and Bubbles*, Monterey, CA, D. H. Le Croissette, Ed., NASA, 392 pp.

Richards, C. N., and G. A. Dawson, 1971: The hydrodynamic instability of water drops falling at terminal velocity in vertical electric fields. *J. Geophys. Res.*, **76,** 3445–3455.